

In closing, it is worthwhile mentioning that the bulk of the computation involved in the present calculation concerned the determination of the electronic R -matrix levels at seven internuclear distances with use of already-existing fixed-nuclei R -matrix codes. The additional work to calculate the vibrational cross sections, which includes the fitting of the potential curves, determination of vibrational eigenstates and vibrational R matrices, and the final matching to the external solutions, was trivial because only two minutes of computing time on the CDC 6600 were needed to calculate the vibrational cross sections at over 100 energies. This enabled us to study the details of the transitions in a way which would be prohibitive with even the most efficient close-coupling technique.

Further details of the calculations will appear in later publications.

The authors are indebted to the staff of the Centre de Calcul de Physique Nucléaire at the University of Paris for the help they have given

us over the past eight months.

^(a)On sabbatical leave from the Los Alamos Scientific Laboratory, Los Alamos, N. M. 87545.

¹B. I. Schneider, M. Le Dourneuf, and P. G. Burke, to be published.

²B. I. Schneider, *Chem. Phys. Lett.* **31**, 237 (1975), and *Phys. Rev. A* **11**, 1957 (1975), and **14**, 1823 (1976); P. G. Burke, I. Mackey, and I. Shimamura, *J. Phys. B* **10**, 249 (1977).

³H. Erhardt and K. Willmann, *Z. Phys.* **204**, 462 (1967).

⁴S. F. Wong, unpublished.

⁵K. Rohr, *J. Phys. B* **10**, 2215 (1977).

⁶N. Chandra and A. Temkin, *Phys. Rev. A* **13**, 188 (1976); A. Temkin, in *Electron and Photon Molecule Collisions*, edited by T. N. Rescigno, B. V. McKoy, and B. I. Schneider (Plenum, New York, 1979).

⁷D. T. Birtwistle and A. Herzenberg, *J. Phys. B* **4**, 53 (1971).

⁸M. Krauss and F. H. Mies, *Phys. Rev. A* **1**, 1592 (1970).

⁹D. Golden, *Phys. Rev. Lett.* **17**, 847 (1966).

¹⁰R. E. Kennerly and R. A. Bonham, *Phys. Rev. A* **17**, 1844 (1978).

Theory of Filament Formation in Self-Focusing Media

S. C. Abbi and Nitin C. Kothari

Department of Physics, Indian Institute of Technology, Hauz Khas, New Delhi 110029, India

(Received 30 August 1979)

The instability theory for sinusoidal perturbations is extended by use of an appropriate energy-conservation criterion. This theory predicts that perturbations initially grow exponentially but can subsequently either stabilize or decay depending on their transverse size.

In situations where intense laser beams traveling through nonlinear cubic media ($\epsilon = \epsilon_0 + \epsilon_2 |\vec{E}|^2$) result in multiple filament formation, there is a one-to-one correspondence¹ between the filaments and intensity spikes riding with the incident laser beams. Instability theories^{2,3} that consider growth of intensity spikes or perturbations predict that they grow exponentially as long as the laser background is not appreciably depleted. Many important experimental facts concerning filament formation remain unexplained. These are stabilization of intensity in spikes (formation of stable waveguidelike filamentary tracks), existence of a well-defined threshold for filament formation, and an almost constant size of filaments in a given nonlinear medium. Some of these facts are adequately explained by the theory of filament formation presented here.

In our theoretical model, similar to that of

Bespalov and Talanov,² we consider a complex perturbation ($e_1 + ie_2$) riding on a uniform background laser optical field $|\vec{E}_0|$. Instead of assuming exponential growth we write the sinusoidal perturbation in the form^{3,4}

$$e_{1,2} = e_{10,10} e^{\alpha(z)} \sin(K_{\perp x} x) \sin(K_{\perp y} y), \quad (1)$$

where $K_{\perp}^2 = K_{\perp x}^2 + K_{\perp y}^2$ relates to the characteristic size of the perturbation and $\alpha(z)$ is the growth parameter which is taken to be a real quantity.

Since both the background and the perturbation have infinite transverse extent, it is useful to consider cells of size $(\pi/K_{\perp x}) \times (\pi/K_{\perp y})$ individually.⁴ Overall conservation implies that energy in each "characteristic cell" should be conserved during propagation. According to Eq. (1) the energy of the perturbation, at distance z , in a char-

acteristic cell is

$$\int_0^{\pi/K_{\perp x}} \int_0^{\pi/K_{\perp y}} |e_1 + ie_2|^2 dx dy = \frac{1}{4}(e_{10}^2 + e_{20}^2) e^{2\alpha(z)} \frac{\pi^2}{K_{\perp x} K_{\perp y}}.$$

This energy is drawn from the initial uniform background energy $|\vec{E}_0|^2(\pi^2/K_{\perp x}K_{\perp y})$. Therefore, the net electric field intensity in the background at distance z is given by $|\vec{E}_0|^2[1 - \frac{1}{4}\delta^2 e^{2\alpha(z)}]$, where $\delta = |e_{10}^2 + e_{20}^2|^{1/2}/|\vec{E}_0|$, which measures the initial perturbation. Replacing $|\vec{E}_0|^2$ by this value in the coupled equations of Bepalov and Talanov,² we obtain a new set of coupled equations for e_1 and e_2 :

$$\nabla_{\perp}^2 e_1 + 2k \frac{\partial e_2}{\partial z} + \frac{2\epsilon_2}{\epsilon_0} k^2 |\vec{E}_0|^2 e_1 - \frac{2\epsilon_2}{\epsilon_0} k^2 \frac{\delta^2}{4} |\vec{E}_0|^2 e^{2\alpha} e_1 = 0, \quad \nabla_{\perp}^2 e_2 - 2k \frac{\partial e_1}{\partial z} = 0. \quad (2)$$

Substituting Eq. (1) into Eq. (2) and eliminating e_1 and e_2 , one would obtain

$$(d\alpha/dz)^2 + a^2 e^{2\alpha} = h_0^2, \quad (3)$$

where

$$a^2 = \frac{K_{\perp}^2}{4k^2} \frac{2\epsilon_2}{\epsilon_0} k^2 |\vec{E}_0|^2 \frac{\delta^2}{4}, \quad (4a)$$

and

$$h_0^2 = \frac{K_{\perp}^2}{4k^2} \frac{2\epsilon_2}{\epsilon_0} k^2 |\vec{E}_0|^2 - K_{\perp}^2. \quad (4b)$$

The quantity h_0^2 is taken to be positive.

To study the growth of the perturbation we solve Eq. (3) for $\alpha(z)$. A trivial solution of Eq. (3) is $\alpha = \ln(h_0/a) = \text{const}$. With initial conditions, $\alpha(z=0) = 0$ and α is an increasing function of z , the nontrivial solution can be written as

$$\alpha(z) = \ln\{(h_0/a) \text{sech}[h_0(z-z_0)]\}, \quad (5)$$

where

$$z_0 = \frac{1}{2h_0} \ln \left[\frac{h_0 + (h_0^2 - a^2)^{1/2}}{h_0 - (h_0^2 - a^2)^{1/2}} \right]. \quad (6)$$

It is easily verified that at $z = z_0$, α is maximum and its value is given by

$$\alpha_{\text{max}} = \ln(h_0/a). \quad (7)$$

This shows that at $z = z_0$, both the solutions coincide. The initial conditions allow us to choose solution (5) for $z \leq z_0$. For $z > z_0$ there are two possible choices: either $\alpha = \ln(h_0/a) = \text{const}$ or α is given by Eq. (5). If α satisfies Eq. (5) for $z > z_0$, it decreases with increasing z values, thereby implying a backflow of energy from the perturbation to the background. To determine condition under which this is possible we let $K_{\perp}^2 = \eta(\epsilon_2/\epsilon_0)k^2|\vec{E}_0|^2$ or $b^2 = \eta^{-1}b_{\text{opt}}^2$, where $b (= \pi/K_{\perp})$ measures the size of the perturbation, b_{opt} is the size of the fastest-growing perturbation as given by Bepalov and Talanov,² and η is a dimensionless parameter that relates them. From Eq. (4)

we obtain $h_0^2/a^2 = (4 - 2\eta)/\delta^2$, and the maximum energy in the perturbation per characteristic cell is given by

$$\begin{aligned} & \frac{1}{4}(e_{10}^2 + e_{20}^2) \exp(2\alpha_{\text{max}}) \\ &= \frac{1}{4} |\vec{E}_0|^2 \delta^2 [(4 - 2\eta)/\delta^2] = |\vec{E}_0|^2 (1 - \frac{1}{2}\eta), \end{aligned} \quad (8)$$

and the corresponding energy in the background per characteristic cell is given by

$$|\vec{E}_0|^2 [1 - \frac{1}{4}\delta^2(4 - 2\eta)/\delta^2] = |\vec{E}_0|^2 \frac{1}{2}\eta. \quad (9)$$

The main background and the perturbation are coupled through the nonlinearity of the medium. The direction of energy transfer between them is determined by their relative energy densities. Initially the main background has larger energy density which leads to the growth of the perturbation. The reverse can also happen. The backflow of energy from the perturbation to the main background⁵ is possible only when the energy per characteristic cell at $z = z_0$ in the perturbation is larger than the corresponding energy in the main background. Equations (8) and (9) imply that $\eta < 1$ for backflow of energy to occur. The quantity h_0^2/a^2 cannot be less than unity since α_{max} would then be negative according to Eq. (7) and this is not commensurate with initial conditions. Since $h_0^2/a^2 = (4 - 2\eta)/\delta^2$, it is implied that $\eta \leq 2 - \frac{1}{2}\delta^2$.

The choice of the solution of $\alpha(z)$ for $z > z_0$ is determined by the value of η (or the size b of the perturbation) as follows:

(i) For $0 < \eta < 1$ (or $b > b_{\text{opt}}$), $\alpha(z)$ is given by solution (5). This is shown in curves I, III, and V of Fig. 1. In this case the perturbation grows in energy to a maximum value (until $z = z_0$) and then decays giving back all the energy to the background. No stable filament formation results.

(ii) For $1 \leq \eta \leq 2 - \frac{1}{2}\delta^2$ [or $b_{\text{opt}}/(2 - \delta^2/2)^{1/2} \leq b \leq b_{\text{opt}}$], the choice of solution for Eq. (3) is $\alpha = \ln(h_0/a) = \text{const}$. This is shown in curves II, IV, and VI of Fig. 1. In this case the perturbation

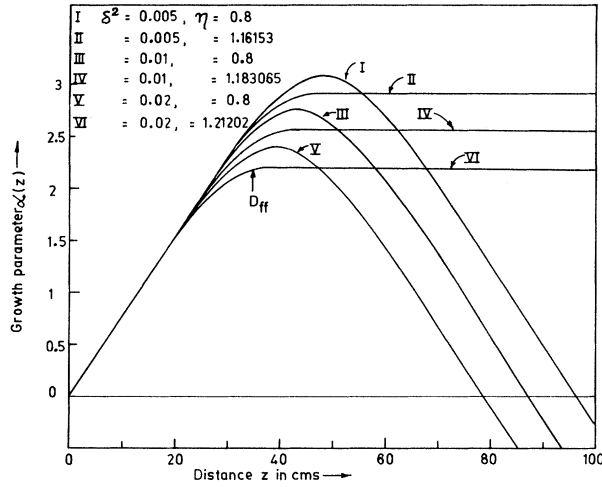


FIG. 1. Growth parameter $\alpha(z)$ plotted for optimum size perturbations traveling with a uniform incident electric field $|\vec{E}_0| = 300$ esu from ruby laser in nitrobenzene. Plots for three values of δ^2 are shown.

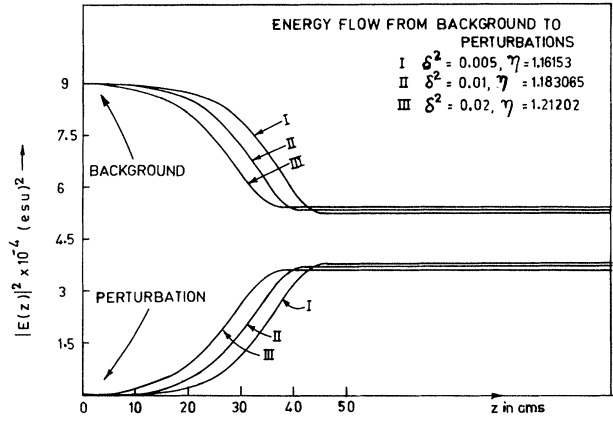


FIG. 2. Plots of energy per characteristic cell as a function of z for the perturbation as well as the background for nitrobenzene. Initial background $|\vec{E}_0|$ is taken to be 300 esu. Plots for 0.5%, 1%, and 2% intensity perturbation are shown.

grows in energy to a maximum value at $z = z_0$ and then stabilizes to form trapped filamentary tracks.

Results of sample calculations, plotted in Fig. 2, indicate that energy in the perturbation always remains smaller than the energy in the background. The ratio of the corresponding intensities is $8/\eta - 4$. Filaments are observable if this ratio is larger than unity indicating that for this, η should be in the range $1 < \eta < 1.6$ or the size b

should be in the range $0.79b_{\text{opt}} < b < b_{\text{opt}}$. This explains the nearly constant size of filaments observed in various experiments.

In order to find threshold for filament formation in terms of the distance for the first appearance of filaments, D_{ff} , we need to find an optimum value of η (or perturbation size) for which z_0 is minimum. For this, we put $dz_0/dK_{\perp} = 0$, which implies that η should satisfy the following equality:

$$\frac{\eta}{\eta - 1} = \left(1 - \frac{\delta^2}{4 - 2\eta}\right)^{1/2} \left\{ \ln \left[1 + \left(1 - \frac{\delta^2}{4 - 2\eta}\right)^{1/2} \right] - \ln \left[1 - \left(1 - \frac{\delta^2}{4 - 2\eta}\right)^{1/2} \right] \right\}, \quad (10)$$

For a particular value of δ^2 (fractional intensity in the perturbation), we can obtain optimum value of η (or optimum size of the perturbation) using Eq. (10). We next obtain h_0 and h_0^2/a^2 using $h_0 = [\eta(2 - \eta)]^{1/2} \frac{1}{2} (\epsilon_2/\epsilon_0) k |\vec{E}_0|^2$ and $h_0^2/a^2 = (4 - 2\eta)/\delta^2$. Using these values of h_0 and h_0^2/a^2 we find D_{ff} from Eq. (6). For those experimental situations where δ^2 is small (or $a^2/h_0^2 \ll 1$), Eq. (6) can be put in an approximate form, given by

$$D_{ff} \approx \frac{2\epsilon_0}{\epsilon_2 k |\vec{E}_0|^2} \ln \left(\frac{A}{\delta^B} \right), \quad (11)$$

where

$$\ln A = \frac{1}{2} [\eta(2 - \eta)]^{-1/2} \ln(16 - 8\eta) \quad (12)$$

and

$$B = [\eta(2 - \eta)]^{-1/2}. \quad (13)$$

Suydam⁴ has found that the experimental values for D_{ff} can be fitted well to an empirical formula

$$D_{ff} = \frac{2\epsilon_0}{\epsilon_2 k |\vec{E}_0|^2} \ln \left(\frac{3}{\delta} \right). \quad (14)$$

Our theoretical result (11) is comparable with the empirical formula (14) as is evident from a tabulation of values for $\ln(A/\delta^B)$ and $\ln(3/\delta)$ in Table I.

By incorporating energy conservation in the theory of instability growth, we are able to explain (a) that for specific range of characteristic sizes, the energy in the perturbation stabilizes to a constant value at a well-defined distance inside the nonlinear medium; (b) that for a specific characteristic size of the perturbation, the distance at which the stabilization takes place is

TABLE I. Comparison of theoretical results [Eq. (11), $\ln(A/\delta^B)$] with empirical results [Eq. (14), $\ln(3/\delta)$].

δ^2	η	A	B	$\ln(3/\delta)$	$\ln(A/\delta^B)$
0.005	1.161 53	2.623	1.013	3.748	3.649
0.01	1.183 065	2.598	1.017	3.401	3.297
0.02	1.212 02	2.565	1.023	3.055	2.944

shortest and this distance compares well with the results of Suydam; and (c) that for stabilized experimentally observable filaments the initial size of the perturbation, b , lies between b_{opt} and $b_{\text{op}}/(1.6)^{1/2}$ (as shown in the text) explaining thereby the nearly constant size of filaments observed ex-

perimentally.

¹S. C. Abbi and H. Mahr, Phys. Rev. Lett. **26**, 604 (1971), and Appl. Phys. Lett. **19**, 415 (1971).

²V. I. Bespalov and V. I. Talanov, Zh. Eksp. Teor. Fiz., Pis'ma **3**, 471 (1966) [JETP Lett. **3**, 307 (1966)].

³K. A. Bruckner and S. Jorna, Phys. Rev. Lett. **17**, 78 (1966).

⁴B. R. Suydam, in *Laser-Induced Damage in Optical Materials*, U. S. National Bureau of Standards Special Publication No. 387, edited by A. J. Glass and A. H. Guenther, (U. S. GPO, Washington, D. C., 1973); B. R. Suydam, IEEE J. Quantum Electron. **10**, 837 (1974).

⁵The backflow of energy into other Fourier components is neglected in this work since the perturbation is assumed to preserve its shape during propagation (aberrationless case). Inclusion of aberrations might change the results quantitatively.

Nonlinear Formulation and Efficiency Enhancement of Free-Electron Lasers

P. Sprangle, Cha-Mei Tang,^(a) and W. M. Manheimer
U. S. Naval Research Laboratory, Washington, D. C. 20375

(Received 11 July 1979)

We present a general, self-consistent, nonlinear theory of the free-electron laser (FEL) process. The formulation of the temporal steady-state problem results in a set of coupled nonlinear FEL equations governing the spatial evolution of the amplitudes and wavelengths of the fields. We show that intrinsic FEL efficiencies can be greatly enhanced by spatially contouring the magnetic pump-field parameters. In the optical regime, the single-pass efficiencies are found to exceed 20%.

The operative mechanism in free-electron lasers (FEL's) is a parametric process in which a long-wavelength pump field interacts with a beam of relativistic electrons.¹⁻⁸ In this paper we take the pump to be a static, periodic, right-handed magnetic field. The frequency of the scattered radiation is given by $\omega \approx (1 + v_z c) \gamma_z^2 v_z (2\pi/l) \approx 4\pi \gamma_z^2 c/l$, where $\gamma_z = (1 + v_z^2/c^2)^{-1/2}$, v_z is the axial beam velocity, and l is the pump period. The possibility of using a two-stage FEL scattering process, in order to reduce the electron energy required for very short output wavelengths, has also been suggested.^{8,9}

Roughly speaking, FEL's can be divided into two categories, depending on the gain of the radiation field. In the low-gain experiments,¹⁰ the radiation field in the interaction region increases only slightly during the passage of the electron beam, while in the high-gain experiments,¹¹⁻¹³ the radiation field e -folds many times in the interaction region. Hence, the low-gain regime is most appropriate for oscillator operation, while high-gain FEL's can be operated as either ampli-

fiers or oscillators.

The main objectives of this work are to present a self-consistent nonlinear formulation of the FEL mechanism and to analyze theoretically some of the concepts necessary to develop efficient, high-power, tunable, FEL radiation sources. Some of the salient features of this theory include (i) a completely arbitrary magnetic pump field (period and amplitude can be functions of axial position), (ii) space-charge effects, (iii) arbitrary polarization of the radiation field, (iv) completely relativistic particle dynamics, and (v) frequency and spatial harmonics in the excited fields. The nonlinear formalism developed for the FEL problem is also applicable to a large class of temporal steady-state convective processes. In this approach, there is no large separation of spatial scale lengths, despite the large spatial scale difference between the wavelength of the scattered field and that of the pump field. This permits numerical solutions for cases where the electron-beam energy is extremely high. Our present treatment does not consider trapped-par-